

the annihilation of p by \bar{p} ; i.e.,

$$A = p \quad \text{and} \quad B = \bar{p}. \quad (109)$$

Another possible test is to compare the branching ratios, or detailed distributions, of the radiative decays of any resonance with that of its C -conjugate state. If H_γ violates C, T invariance, then the distribution and branching ratio of, say,

$$N^{*0} \rightarrow p + \pi^- + \gamma \quad (110)$$

may be different from that of

$$\bar{N}^{*0} \rightarrow \bar{p} + \pi^+ + \gamma. \quad (111)$$

From CPT invariance, such a difference can occur only if the strong final-state interaction is not neglected.

ACKNOWLEDGMENTS

We wish to thank Professor P. Franzini, Professor M. Schwartz, and Professor C. S. Wu for discussions.

Antiproton Annihilation in Hydrogen at Rest. I. Reaction $\bar{p} + p \rightarrow K + \bar{K} + \pi$ *

N. BARASH, P. FRANZINI,|| L. KIRSCH, D. MILLER,† J. STEINBERGER,‡ AND T. H. TAN§
Columbia University, New York, New York

AND

R. PLANO

Rutgers, The State University, New Brunswick, New Jersey

AND

P. YAEGER

University of California, San Diego, La Jolla, California

(Received 11 May 1965)

In a study of 735 000 antiproton annihilations at rest in the hydrogen bubble chamber, 182 examples of the reaction $\bar{K}_1 K_1 \pi^0$ and 851 examples of the reaction $K_1 \bar{K}^2 \pi^*$ were recorded. The distributions in the internal variables of these reactions are presented. A substantial fraction of the latter reaction proceeds through an intermediate K^* state; $\bar{p} + p \rightarrow K + K^*$. The theory of the interference effects in this reaction is presented and compared with the experimental result. It is concluded that the KK^* annihilation proceeds dominantly from the $^3S, I=1$ state of the $\bar{N}N$ system. The fraction of $\bar{p}p$ annihilations into KK^* is given as $f_{KK^*} = (2.1 \pm 0.3) \times 10^{-2}$.

I. INTRODUCTION

IN the domain of strong-interaction physics, anti-nucleon-nucleon annihilation has several features which may lead one to hope that the study of these reactions may provide useful information. In particular, the nucleon number is zero, the capture at rest is known to proceed dominantly ($\sim 99\%$) from an S state; hence the parity is negative and the charge-conjugation eigenvalue is linked to the angular momentum [$C(^3S) = -1, C(^1S) = +1$]. Nevertheless, there is not a large amount of published experimental information on the details of the various capture channels, nor has there been a great deal of theoretical interest.

This paper is the first of several contemplated articles in which we intend to present the results of a study

pursued by the Columbia-Rutgers groups on \bar{p} annihilations in a liquid-hydrogen chamber, using an exposure at the Brookhaven National Laboratory AGS machine.

We present the results on the $K\bar{K}\pi$ annihilations. The following reactions are possible:

$$\bar{p} + p \rightarrow K^0 + \bar{K}^0 + \pi^0, \quad (1)$$

$$\bar{p} + p \rightarrow K^0 + K^- + \pi^+, \quad (2)$$

$$\bar{p} + p \rightarrow K^+ + \bar{K}^0 + \pi^-. \quad (3)$$

Reaction (1) can be further separated on the basis of the decay of the kaon:

$$K_1^0 + K_1^0 + \pi^0, \quad (1a)$$

$$K_2^0 + K_2^0 + \pi^0, \quad (1a')$$

$$K_1^0 + K_2^0 + \pi^0. \quad (1b)$$

Reaction (1a') is not observed because of the long K_2 lifetime, but is presumably identical with reaction (1a). Reaction (1b) is, in general, inaccessible to hydrogen-bubble-chamber study because there are two missing

* Work supported in part by the U. S. Atomic Energy Commission.

|| On leave from Brookhaven National Laboratory, Upton, New York.

† Present address: Massachusetts Institute of Technology, Cambridge, Massachusetts.

‡ Present address: CERN, Geneva, Switzerland.

§ Present address: Stanford University, Stanford, California.

neutral particles; however, it is possible at least to learn the extent of K^* formation in this reaction.

As will be seen, K^* formation accounts for a substantial fraction of some of these reactions. We therefore include in this paper a study of the interference phenomena in the process $\bar{p} + p \rightarrow K^* + K$.

II. EXPERIMENTAL PROCEDURE

The hydrogen chamber used in these experiments was designed and constructed at Columbia University. It is 30 in. in diameter, 14 in. deep, and operates in a magnetic field of 14 kG. It was exposed to a separated beam of antiprotons at the BNL AGS machine. The beam was transported at 800 MeV/c, and a carbon absorber inserted immediately in front of the chamber in an amount ($10\frac{1}{4}$ in.) to maximize the rate of stopped \bar{p} in the center of the chamber. Approximately 600 000 pictures were obtained, accounting for 735 000 stopped antiprotons.

The pictures were scanned twice for V 's associated with stoppings. All such pictures were measured with an accuracy of 80μ in the projected full-size view. Of these measurements 91% survived the geometrical reconstruction program. No attempt was made to

recover the failures, which are attributed to inadequacies in the measurements of the events.

The measurements were then tested for kinematical consistency with the reactions (1) to (3), using the program "GRIND" developed at CERN.¹ All events

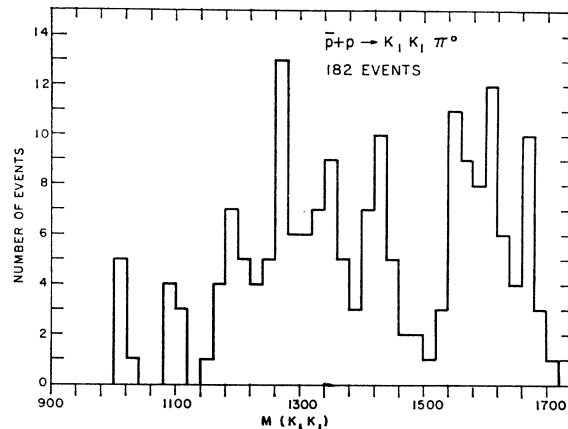


FIG. 3. $(K_1 K_1)$ effective mass distribution from the reaction $\bar{p} + p \rightarrow K_1 + K_1 + \pi^0$.

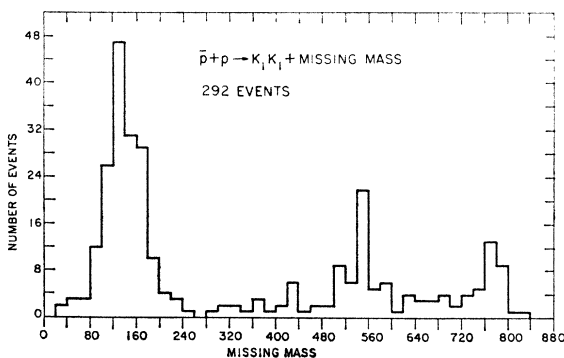


FIG. 1. Missing mass distribution from the reaction $\bar{p} + p \rightarrow K_1 + K_1$ missing mass.

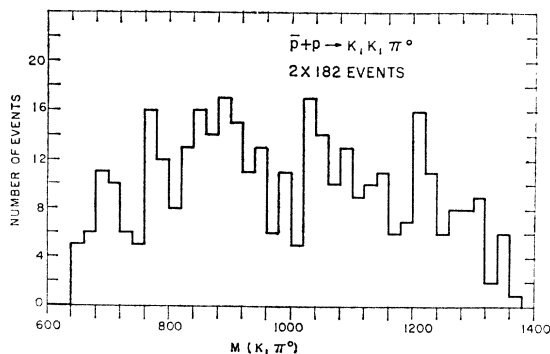


FIG. 2. $(K_1 \pi^0)$ effective mass distribution from the reaction $\bar{p} + p \rightarrow K_1 + K_1 + \pi^0$.

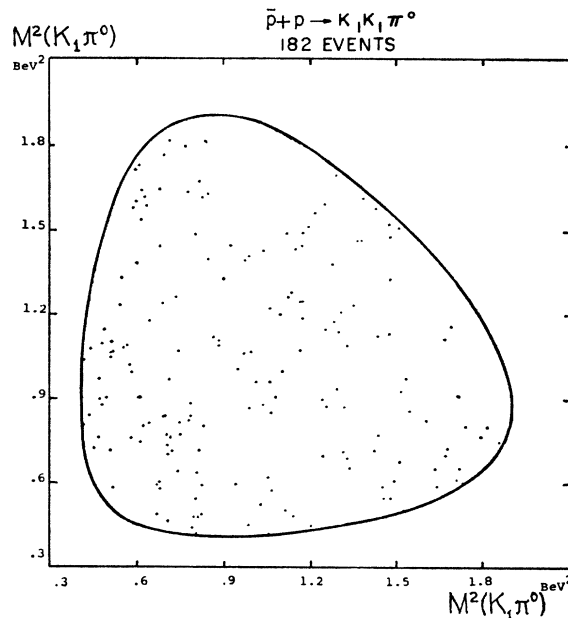


FIG. 4. Dalitz plot for the reaction $\bar{p} + p \rightarrow K_1 + K_1 + \pi^0$.

with $\chi^2 < 5 \times$ (the number of constraints) were retained. Of 379 events consisting of two V 's and no charged tracks associated with the vertex, 182 were consistent with the reaction (1a). Of 6208 events of the type $V + 2$ charged tracks, 438 were consistent with reaction (2), and 413 with reaction (3).

¹ CERN Report No. 3437 (unpublished).

III. RESULTS

A. Invariant Mass Distribution

The mass spectra and Dalitz plots of these events are presented in Figs. 1 to 8. We have combined the data of reactions (2) and (3) since they are consistent with being identical, and are expected to be so on the basis of charge-conjugation invariance. In addition, we present in Fig. 9 the spectrum in the missing mass for all events which show a single K^0 , and no charged tracks at the vertex.

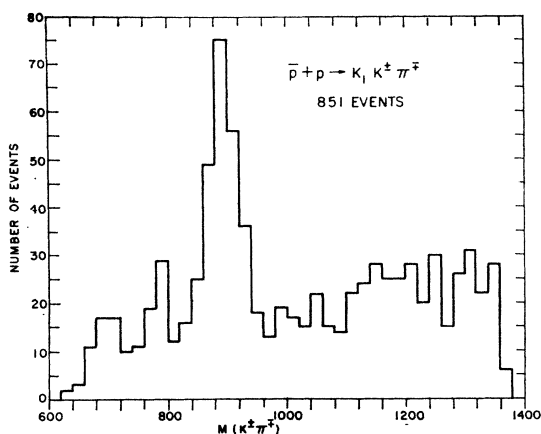


FIG. 5. $(K^\pm\pi^\mp)$ effective mass distribution from the reaction $\bar{p}+p \rightarrow K_1+K^\pm+\pi^\mp$.

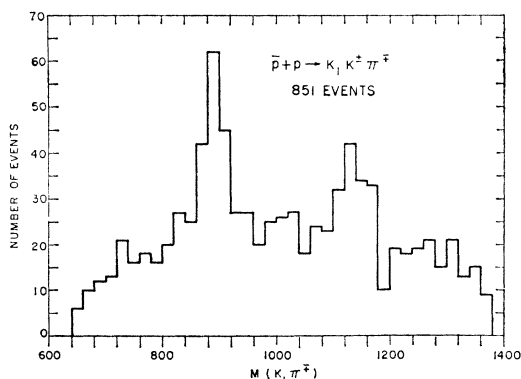


FIG. 6. $(K_1\pi^\mp)$ effective mass distribution from the reaction $\bar{p}+p \rightarrow K_1+K^\pm+\pi^\mp$.

B. Branching Ratios

In order to arrive at the fraction of $\bar{p}p$ annihilation into a particular channel, we make use of the following efficiencies:

- (1) Scanning efficiency 0.95 ± 0.05 .
- (2) Survival probability of event in measurement 0.91 ± 0.03 .
- (3) K_1 decay probability in the chamber 0.91 ± 0.03 . There is a loss of $\sim 1\%$ because the available path length is finite, and about 8% because very short decay

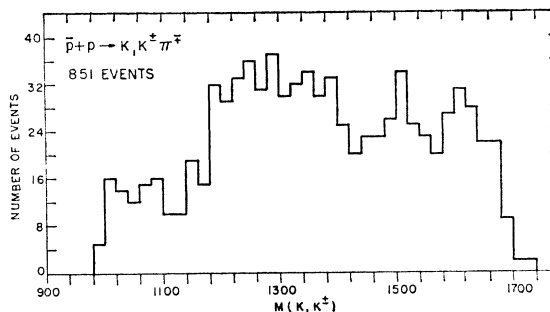


FIG. 7. $(K_1K)^\pm$ effective mass distribution from the reaction $\bar{p}+p \rightarrow K_1+K^\pm+\pi^\mp$.

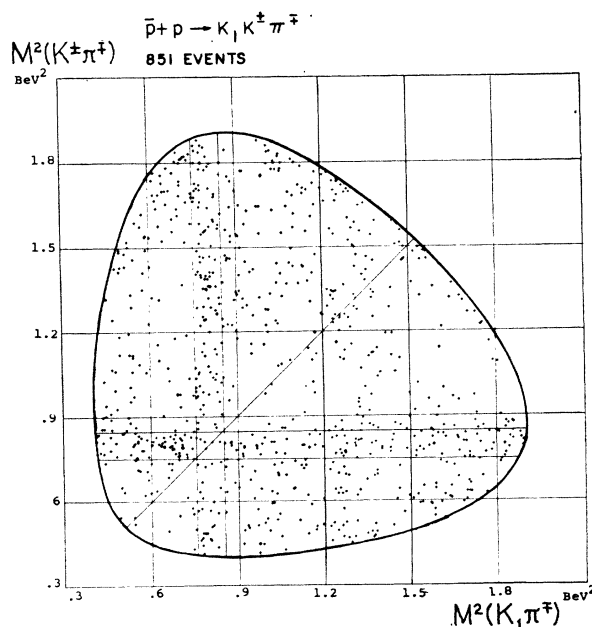


FIG. 8. Dalitz plot for the reaction $\bar{p}+p \rightarrow K_1+K^\pm+\pi^\mp$.

paths ($\sim < 1.5$ mm) are missed. This efficiency depends on the K^0 momentum, but we feel that our statistical accuracies do not warrant this refinement.

(4) Probability of charged decay of K_1^0 , 0.70 ± 0.02 .

(5) Probability of acceptance of the event within the χ^2 limit of five times the number of constraints, 0.99 ± 0.01 .

The total number of \bar{p} stoppings was found to be $(0.735 \pm 0.07) \times 10^6$.

The 182 events of reaction (1a) then represent the fraction $f_{K_1K_1\pi^0} = (0.73 \pm 0.1) \times 10^{-3}$ of all annihilations. The $K_2K_2\pi^0$ rate must be the same, so³ $f_{K_1^2K_1^2\pi^0} = (1.46 \pm 0.2) \times 10^{-3}$. The 851 events of reactions (2) and (3) account for the fraction $f_{K^0K^\pm\pi^\mp} = (4.25 \pm 0.55)$

² M. Chretien *et al.*, Brandeis-Brown-Harvard-Massachusetts Institute of Technology Collaboration, Phys. Rev. **131**, 2208 (1963).

³ With the notation $K_1^2K_1^2\pi^0$ we mean either $K_1K_1\pi^0$ or $K_2K_2\pi^0$, but not $K_1K_2\pi^0$.

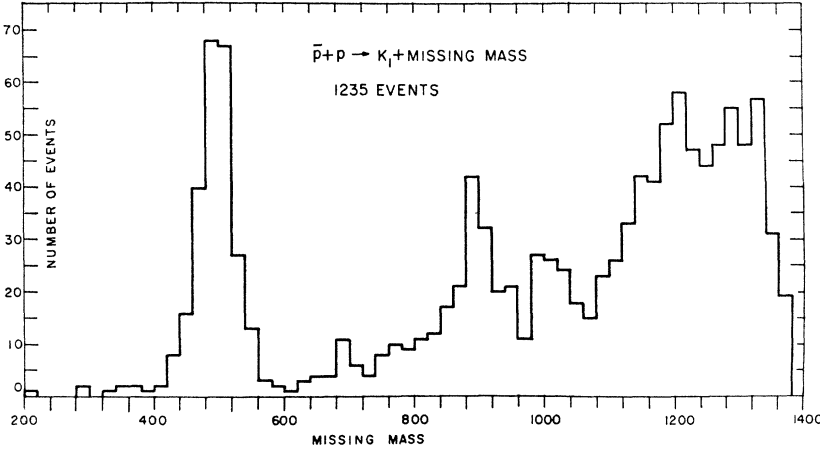


FIG. 9. Missing mass distribution from the reaction $\bar{p}+p \rightarrow K_1 + \text{missing mass}$.

$\times 10^{-3}$. The errors include an estimated 10% error in the total antiproton stoppings. This error should not be applied in a comparison of rates.

C. K^* Production

Within the statistical resolution of the experiment there is no K^* production in the $K_1^2 K_1^2 \pi^0$ channel.³ However, the missing mass plot of Fig. 9 shows a distinct K^{0*} peak of 70 ± 15 events corresponding to a branching ratio of $(0.175 \pm 0.04) \times 10^{-3}$ for the channel $K_1 K^{0*}$, $K^{0*} \rightarrow K_2^0 + \pi^0$. In addition, an equal number are expected in the channel $K_2 K_1^*$, $K_1^* \rightarrow \pi^0 + K_1^0$, which is not detected. So, $f_{K_1^2 K_2^1, K_2^1 \rightarrow K_2^1 + \pi^0} = (0.35 \pm 0.08) \times 10^{-3}$.

The mass distributions of reactions (2) and (3) yield

$$170 \pm 25 \text{ events, } K^{0*} \rightarrow K^\pm + \pi^\mp$$

and

$$113 \pm 20 \text{ events, } K^{\pm*} \rightarrow K_1^0 + \pi^\pm.$$

This corresponds to

$$f_{K_1^2 K^{0*}, K^0 \rightarrow K^\pm + \pi^\mp} = (0.85 \pm 0.16) \times 10^{-3}$$

and

$$f_{K^{\pm*} K^\mp, K^\mp \rightarrow K_1^2 + \pi^\mp} = (0.566 \pm 0.12) \times 10^{-3}.$$

IV. THEORY OF THE ANNIHILATION

$$\bar{p} + p \rightarrow K + K^*$$

We assume that the capture proceeds from the 3S state. The reaction may then be classified into four channels according to isotopic spin and angular momentum:

$$^3S(I=0), \quad (4a)$$

$$^3S(I=1), \quad (4b)$$

$$^1S(I=0), \quad (4c)$$

$$^1S(I=1). \quad (4d)$$

The 3S and 1S captures are incoherent with respect to each other, at least after integration over space. The four KK^* charge states which have the same quantum

numbers of isotopic spin and charge conjugation are

$$\frac{1}{2}[(K^+ K^{-*} - K^0 \bar{K}^{0*}) + (K^- K^{+*} - \bar{K}^0 K^{0*})], \quad (5a)$$

$$\frac{1}{2}[(K^+ K^{-*} + K^0 \bar{K}^{0*}) + (K^- K^{+*} + \bar{K}^0 K^{0*})], \quad (5b)$$

$$\frac{1}{2}[(K^+ K^{-*} - K^0 \bar{K}^{0*}) - (K^- K^{+*} - \bar{K}^0 K^{0*})], \quad (5c)$$

$$\frac{1}{2}[(K^+ K^{-*} + K^0 \bar{K}^{0*}) - (K^- K^{+*} + \bar{K}^0 K^{0*})], \quad (5d)$$

where we use the convention

$$CK^0 = \bar{K}^0,$$

$$CK^{0*} = -\bar{K}^{0*}.$$

We consider the annihilation into a particular charge channel, $K^+ \bar{K}^0 \pi^-$. The amplitudes are

$$[K^+(\bar{K}^0 \pi^-) - \bar{K}^0(K^+ \pi^-)], \quad (6a)$$

$$[K^+(\bar{K}^0 \pi^-) + \bar{K}^0(K^+ \pi^-)], \quad (6b)$$

$$[K^+(\bar{K}^0 \pi^-) + \bar{K}^0(K^+ \pi^-)], \quad (6c)$$

$$[K^+(\bar{K}^0 \pi^-) - \bar{K}^0(K^+ \pi^-)]. \quad (6d)$$

The parenthesis indicates that the system is resonant, that is, the matrix element will have the Breit-Wigner denominator in the corresponding variables.

In order to write the space functions we use the following notation:

p = 4-momentum of $\bar{p}p$ system,

S = polarization 4-vector of $\bar{p}p$ system for 3S state,

k = 4-momentum of K^* ,

e = polarization 4-vector of K^* ,

q = 4-momentum of pion,

$$D_+ = [(M_{K^+ \pi^-} - M_{K^*}) + (i\Gamma_{K^*}/2)],$$

$$D_0 = [(M_{K^0 \pi^0} - M_{K^*}) + (i\Gamma_{K^*}/2)],$$

and $M_{K\pi}$ is the invariant mass of the $K\pi$ system.

$$\epsilon_\mu k_\mu = S_\mu p_\mu = 0.$$

The matrix elements for the transition $\bar{p}p \rightarrow K + K^*$,

$K^* \rightarrow K + \pi$ can then be written

$$M_{1S} \propto \sum_{K^* \text{ spin}} \frac{e_\mu \hat{p}_\mu e_\nu q_\nu}{D} \propto \frac{\mathbf{q} \cdot \mathbf{k}}{D},$$

where \mathbf{q} is the momentum of the pion in the K^* c.m. system and \mathbf{k} is the momentum of the K^* in the $\bar{p}p$ c.m. system.

$$M_{3S} \propto \sum_{K^* \text{ spin}} \frac{\epsilon^{\alpha\beta\gamma\delta} p_\alpha S_\beta k_\gamma e_\delta e_\mu q_\mu}{D} = \frac{\epsilon^{\alpha\beta\gamma\delta} p_\alpha S_\beta k_\gamma q_\delta}{D} \propto \frac{\mathbf{S} \cdot \mathbf{q} \times \mathbf{k}}{D} \text{ in } \bar{p}p \text{ c.m. system.}$$

The matrix elements for the transitions (6a)–(6d) are then

$$M_a \propto \mathbf{S} \cdot \left[\frac{\mathbf{q}_0 \times \mathbf{k}_0}{D_0} - \frac{\mathbf{q}_+ \times \mathbf{k}_+}{D_+} \right],$$

$$M_b \propto \mathbf{S} \cdot \left[\frac{\mathbf{q}_0 \times \mathbf{k}_0}{D_0} + \frac{\mathbf{q}_+ \times \mathbf{k}_+}{D_+} \right],$$

$$M_c \propto \left[\frac{\mathbf{q}_0 \cdot \mathbf{k}_0}{D_0} + \frac{\mathbf{q}_+ \cdot \mathbf{k}_+}{D_+} \right],$$

$$M_d \propto \left[\frac{\mathbf{q}_0 \cdot \mathbf{k}_0}{D_0} - \frac{\mathbf{q}_+ \cdot \mathbf{k}_+}{D_+} \right],$$

where \mathbf{k}_0 and \mathbf{k}_+ are the three-momenta of the $K^0\pi^-$ and $K^+\pi^-$ systems, respectively, in the $\bar{p}p$ c.m. system, and \mathbf{q}_0 and \mathbf{q}_+ are the pion momenta in the $K^0\pi^-$ and $K^+\pi^-$ c.m. systems, respectively. For the intensity distributions we can finally write after averaging over the initial polarization in the 3S case:

$$^3S, I=0: \left| \frac{\mathbf{q}_0 \times \mathbf{k}_0}{D_0} - \frac{\mathbf{q}_+ \times \mathbf{k}_+}{D_+} \right|^2, \quad (7a)$$

$$^3S, I=1: \left| \frac{\mathbf{q}_0 \times \mathbf{k}_0}{D_0} + \frac{\mathbf{q}_+ \times \mathbf{k}_+}{D_+} \right|^2, \quad (7b)$$

$$^1S, I=0: \left| \frac{\mathbf{q}_0 \cdot \mathbf{k}_0}{D_0} + \frac{\mathbf{q}_+ \cdot \mathbf{k}_+}{D_+} \right|^2, \quad (7c)$$

$$^1S, I=0: \left| \frac{\mathbf{q}_0 \cdot \mathbf{k}_0}{D_0} - \frac{\mathbf{q}_+ \cdot \mathbf{k}_+}{D_+} \right|^2. \quad (7d)$$

Note that (7a) and (7b) can be modified slightly in a way so that the sign of the interference effect is more clearly exhibited:

$$^3S, I=0: \left| \frac{1}{D_0} + \frac{1}{D_+} \right|^2 (\mathbf{Q} \times \mathbf{k})^2, \quad (7a')$$

$$^3S, I=1: \left| \frac{1}{D_0} - \frac{1}{D_+} \right|^2 (\mathbf{Q} \times \mathbf{k})^2. \quad (7b')$$

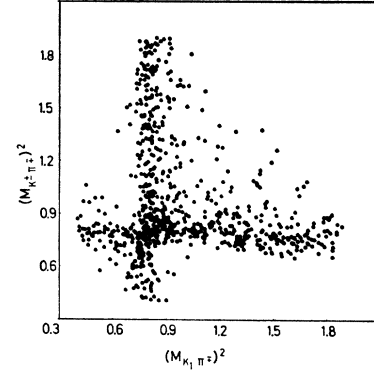


FIG. 10. Monte Carlo calculation for $\bar{p}p$ annihilation in the $^3S I=0$ state into the channel $K+K^* \rightarrow K^0+K^\pm+\pi^\mp$ (case a).

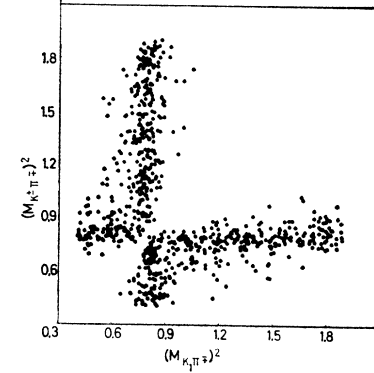


FIG. 11. Monte Carlo calculation for $\bar{p}p$ annihilation in the $^3S I=1$ state into the channel $KK^* \rightarrow K^0+K^\pm+\pi^\mp$ (case b).

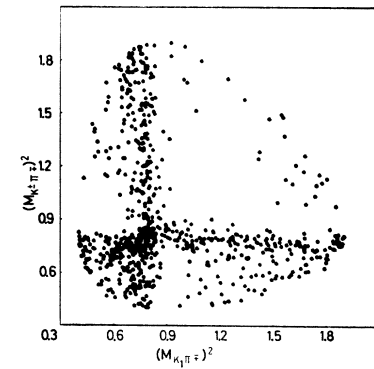


FIG. 12. Monte Carlo calculation for $\bar{p}p$ annihilation in the $^1S I=0$ state into the channel $KK^* \rightarrow K^0+K^\pm+\pi^\mp$ (case c).

Here \mathbf{Q} is the pion momentum in the $\bar{p}p$ c.m. system and \mathbf{k} is the momentum of either kaon.

The distributions (7a)–(7d) are functions of m_0 and m_- only. The charge-conjugate channel has the same distributions, if charge-conjugation invariance is granted. The expressions (7a) to (7d) have been evaluated using Monte Carlo techniques and are presented in Figs. 10 to 13. In addition, we may point out that the distribution in the $K^0K^0\pi^0$ channel is given by

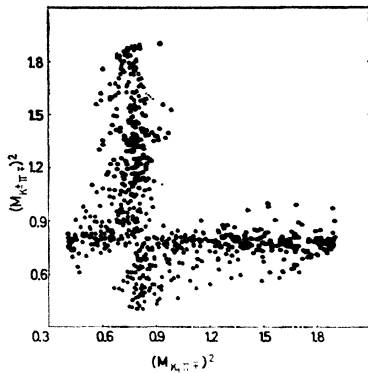


FIG. 13. Monte Carlo calculation for $\bar{p}p$ annihilation in the ${}^1S\ I=1$ state into the channel $KK^* \rightarrow K^0 + K^\pm + \pi^\mp$.

(7a) for 3S capture, and as already noted, will be a state $K_1K_2\pi^0$. The interference at the K^*K^* crossing is negative. The distribution for 1S capture is given by (7c) with positive interference.

V. DISCUSSION OF THE RESULTS

The experimental Dalitz plot of Fig. 8 has two striking features: (a) There are prominent K^* bands, which account for one-third of the events, and (b) there is a concentration of events along the boundary of the Dalitz plot.

We have reached no understanding of this latter effect, and proceed to the discussion of the K^* bands in the reaction $\bar{p} + p \rightarrow K + K^*$. We try to understand the experimental data on the assumption that the reaction proceeds dominantly in one of the four channels, and try to find this channel.

In the first place, we note that $K_1(K_1\pi^0)$ is absent, but $K_1(K_2\pi^0)$ is present. The charge conjugation of the dominant capture state is therefore negative, and must be 3S . It remains to decide whether the isospin is 1 or 0. The most striking difference between the two expectations is the fact that the $I=1$ state shows negative interference, whereas the isospin-0 state shows positive interference at the crossing point of the K^* bands (Figs. 10 and 11). The experimental data are not as clear on this point as one might like; however, the crossing region shows a depletion in the number of events from which we conclude that $I=1$. The adjacent region shows a depletion in the $K^{\pm*}$ at low $K^\pm\pi^\mp$ mass, and a reinforcement in the K^{0*} at small $K^0\pi^\pm$ mass. We interpret this in the following way. There is a considerable nonresonant background. It is not known how this is divided between 3S and 1S , but if we take only one-half in the 3S , we arrive at a background amplitude which is approximately one-third as large

TABLE I. Expected and observed KK^* annihilation rates in the several charge channels.

Charge channel	Expected rate (relative)	Observed fraction
$K^\pm[K^\mp\pi^0]$	1	Not observed
$K^0[K^0\pi^0]$	1	$(0.35 \pm 0.08) \times 10^{-3}$
$K^0[K^\pm\pi^\mp]$	2	$(0.85 \pm 0.16) \times 10^{-3}$
$K^\pm[K^0\pi^\mp]$	2	$(0.57 \pm 0.12) \times 10^{-3}$

as the average within the K^* bands and which interferes with the KK^* amplitude. In the K -band crossing region, the background amplitude may be expected to be reasonably constant, whereas the K^* amplitude in the ${}^3S\ I=1$ state changes sign on reflection about the diagonal of Fig. 8. The enhancement on the K^{0*} side and the depletion on the $K^{\pm*}$ side are then due to positive interference with the background, an interference which has the opposite sign for the two. We also see in this a means to understand the difference in the total K^{0*} and $K^{\pm*}$ production in this channel. We note that the assignment of $I=1$ for the state chiefly responsible for the KK^* annihilation leads to the prediction that this channel will be twice as strong in $n\bar{p}$ annihilation as in $\bar{p}p$ annihilation.

The model also predicts the distribution among the various charge channels. These expectations are the same for the four capture states. The expectations, together with the results, are presented in Table I. Except for the asymmetry discussed above, the expectations are fulfilled within experimental error.

If we also allow for the unobserved channel, we find for the total fraction of the annihilation into the state KK^* , $f_{KK^*} = (2.1 \pm 0.3) \times 10^{-3}$.

ACKNOWLEDGMENTS

We would like to thank those who have helped us in these efforts: Dr. A. Prodell and the crew of the 30-in. hydrogen chamber as well as the staff of the Brookhaven AGS machine for the exposure; Professor D. Colley and Dr. A. Prodell for the chamber design and construction; Dr. C. A. Steinberger and Dr. D. Berley for the design and putting into operation of the separated beam, as well as the technicians at the Nevis and Rutgers laboratories who carried out the search for, and the measurement of, the events. One of us (J. S.) would like to acknowledge helpful discussions with Dr. J. S. Bell, Dr. N. Cabibbo, Dr. W. Fraser, and Dr. M. Veltman, as well as the hospitality of the University of California (San Diego) at La Jolla, and CERN. Another of us (P. F.) would like to thank Professor G. Feinberg and Professor M. Dresden for discussions.